Global Alfvén modes: Theory and experiment*

A. D. Turnbull,† E. J. Strait, W. W. Heidbrink,[a] M. S. Chu, H. H. Duong,[a] J. M. Greene, L. L. Lao, T. S. Taylor, and S. J. Thompson
General Atomics, San Diego, California 92186-9784

(Received 18 December 1992; accepted 31 March 1993)

It is shown that the theoretical predictions and experimental observations of toroidicity-induced Alfvén eigenmodes (TAE's) are now in good agreement, with particularly detailed agreement in the mode frequencies. Calculations of the driving and damping rates predict the importance of continuum damping for low toroidal mode numbers and this is confirmed experimentally. However, theoretical calculations in finite-β, shaped discharges predict the existence of other global Alfvén modes, in particular the ellipticity-induced Alfvén eigenmode (EAE) and a new mode, the beta-induced Alfvén eigenmode (BAE). The BAE mode is calculated to be in or below the same frequency range as the TAE mode and may contribute to the experimental observations at high β. Experimental evidence and complementary analyses are presented confirming the presence of the EAE mode at higher frequencies.

I. INTRODUCTION

Global Alfvén modes, such as the toroidicity-induced Alfvén eigenmode[1] (TAE) are of considerable concern to fusion experiments since they can be driven resonantly unstable by energetic α particles provided certain criteria are met.[2] The first estimates[2] of the destabilization of TAE modes predicted low thresholds in the α-particle β required to overcome stabilization by electron Landau damping. Later experiments[3,4] with beam-driven TAE modes, showed that the original stability estimates underestimated the damping by roughly an order of magnitude. Nevertheless, it became clear that these modes could still be dangerous for ignition experiments and, moreover, could have serious consequences for neutral-beam-heated experiments.[5]

Other global Alfvén modes have also been predicted and actually have a rather longer history than the TAE mode. Gaps in the stable magnetohydrodynamic (MHD) continuum spectrum induced by elongation of the plasma cross section were first noted[6,7] in the 1970s. Global "kink" modes embedded in the stable spectrum were also noted,[7] but the actual elongation-induced Alfvén eigenmode (EAE) associated with the gap was not predicted until recently.[8] On the other hand, the so-called global Alfvén eigenmodes (GAE's) were unexpectedly discovered in Alfvén wave heating simulations and experiments as peaks in the antenna impedance at frequencies below the associated continua.[9] The theory was soon developed[10] and the possibility of energetic α-particle destabilization was recognized.[11] However, it was later shown by Fu and Van Dam[2] that toroidal effects would enhance the damping of GAE modes. TAE modes were considered to be more dangerous[2] and little consideration has since been paid to GAE modes, despite the fact that it is now clear that TAE modes are also more strongly damped than the original estimates suggested.

Much of the recent work on the theory of TAE modes has focused on developing damping mechanisms which could account for the original discrepancy with the experiments. The most important of these appear to be ion Landau damping,[12] including an additional resonance[12] at one third the Alfvén speed, continuum damping,[13,14] and coupling of the TAE mode to nearby kinetic Alfvén waves.[15] Inclusion of these effects has been found to provide much more satisfactory agreement between predicted and observed thresholds.[16] However, all the recent theories are essentially restricted to low β, circular cross section, and large aspect ratio, and can only be expected to provide gross quantitative agreement. Chu *et al.*[17] have shown that noncircular shaping and finite β complicate the gap structure considerably, creating, respectively, the EAE gap at frequencies above the TAE gap and a new β-induced "zeroth gap"[17] below it. Except for a few calculations of electron Landau[18] and continuum damping rates,[19,20] neither finite β nor noncircularity have been included in any comprehensive damping estimates.

The major accomplishments of the work presented here are twofold. First, the current state of agreement between the detailed theories and the experimental observations of TAE modes is demonstrated. In particular, multiple TAE modes are both predicted and observed. Because of the complicated dependence of the damping rates on the details of the stable spectrum, an accurate representation of the complete real frequency spectrum is also found to be a useful guide for interpreting the stability estimates. Second, two important new results are described as part of this work: a new global Alfvén mode, the beta-induced Alfvén eigenmode (BAE), which exists in the β-induced gap, is exhibited and the first definitive experimental evidence for the EAE in DIII-D is presented. The existence of these two modes has important consequences for future beam- and α-heated experiments since extrapolations of fast particle instability thresholds to such devices will need to include these new modes.

In the first part of the following section, the experimental and computational analysis tools used to determine

*Paper 4I5, Bull. Am. Phys. Soc. **37**, 1438 (1992).
†Invited speaker.
[a]Permanent address: University of California, Irvine, California 92717.

 0899-8221/93/5(7)/2546/8/$6.00

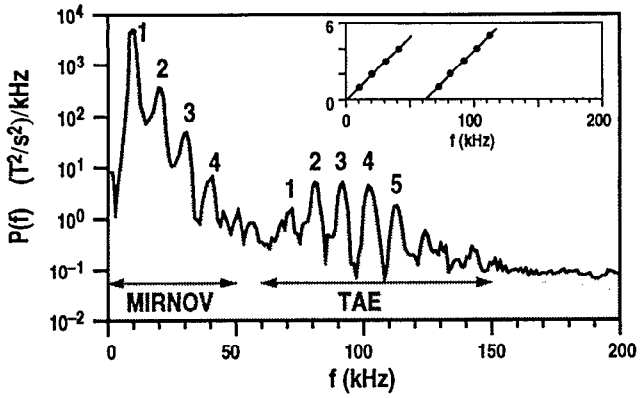

FIG. 1. TAE dB_θ/dt power spectrum versus frequency and toroidal mode number n versus frequency (inset).

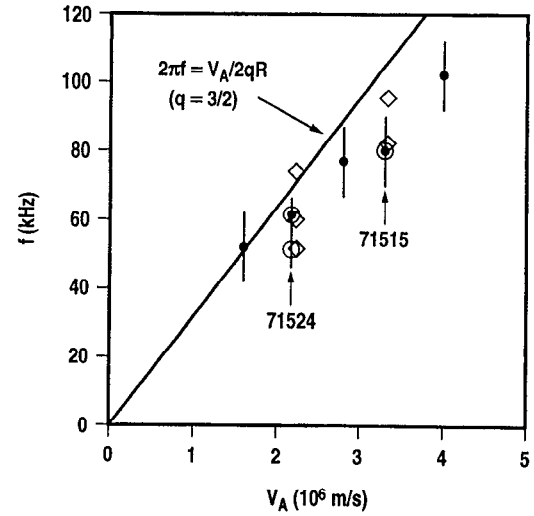

FIG. 2. TAE frequency dependence on v_A. Observed and calculated frequencies from a sequence of L-mode discharges with total current $I_p=0.6$ MA, neutral beam power $P_{NB}=5$ MW, density $n_e=3\times10^{13}$ cm^{-3}, and increasing toroidal magnetic field. The experimentally observed frequencies are shown as small solid dots; high resolution analysis for discharges 71515 and 71524 is shown as the larger open circles. The frequencies computed by GATO are shown as open diamonds.

the real frequencies are described briefly and the detailed agreement between the measured and calculated frequencies is established. In Sec. II B, the various theories for TAE mode damping are applied to DIII-D and the possibility of control of TAE modes by direct modification of the gap structure is shown. In Sec. III, the existence of BAE modes in the same frequency range as the TAE modes is demonstrated. The evidence for the existence of the EAE is presented in Sec. IV. Finally, the conclusions are summarized in Sec. V.

II. TAE MODES: THEORY AND EXPERIMENT

A. Real frequency

In Doublet-III-D (DIII-D),[21] the observed neutral-beam-driven TAE modes are exhibited as finite frequency magnetic perturbations on experimental magnetic probes,[3] generally in the range 50–150 kHz, with toroidal mode numbers in the range $2\leqslant n\leqslant 10$. In contrast, the plasma rotation frequency is generally around 10–20 kHz. Also, the more usual MHD activity in DIII-D, which is generally attributed to fishbone and tearing modes, is observed at frequencies below 50 kHz.

Figure 1 shows the power spectrum for magnetic fluctuations in a typical discharge in which the TAE modes are observed. The discrete peaks in the range 50 kHz $< f \lesssim 150$ kHz correspond to TAE modes with increasing toroidal mode numbers n, Doppler shifted by n times the plasma rotation frequency.[3] Extrapolation to $n=0$ then gives the frequency in the plasma frame as shown in the inset. The inferred Doppler shift is also in good agreement with charge-exchange recombination spectroscopy (CER) measurements of the plasma rotation speed in the range $1\lesssim q\lesssim 2$.

The observed mode frequencies are found to scale linearly with the Alfvén speed v_A as expected for TAE modes. A series of experiments was performed with equal input beam power at increasing toroidal field and the resulting mode frequencies, obtained as described above, are shown in Fig. 2. The scaling with v_A is clearly seen. The line shown at $f=v_A/4\pi qR$, corresponding to $q=1.5$, is the frequency predicted by the earliest theories.[1,2] Note that the observed frequencies do not fit the weak scaling with v_A expected for kinetically destabilized ballooning modes[22](KBM's).

Two discharges in the toroidal field scan have been analyzed in detail: discharges 71515 and 71524. A more refined examination of the experimentally observed spectrum for discharge 71524 revealed that the TAE peaks could be resolved into several sets of peaks corresponding to slightly different frequencies in the plasma frame. These frequencies are also shown in Fig. 2. In the other case (discharge 71515), the TAE activity was relatively weak and no clear evidence of multiple TAE modes could be found.

To obtain a more detailed comparison with the theory, the CONT code[17] is employed to map out the stable continua and gap structures. The ideal MHD stability code GATO[23] is then used to compute eigenmodes in the stable spectrum. The computational mesh in the GATO code discretizes the continua; this allows individual continuum modes to be counted. Note that the variational formulation avoids the necessity of explicitly dealing with jump conditions[13] at the resonant points. Finite damping can be expected to modify the computed eigenfunctions by a correction of order γ/ω in the vicinity of the shear Alfvén resonances, where γ/ω is the ratio of the damping rate to the real frequency. Except in a few special cases, this is not generally estimated in the present work, but these and other estimates typically find γ/ω to be of the order of a few percent so that the neglect of the imaginary part is a reasonably accurate approximation.

A crucial step in obtaining good quantitative agreement between the theory and experiment is in obtaining

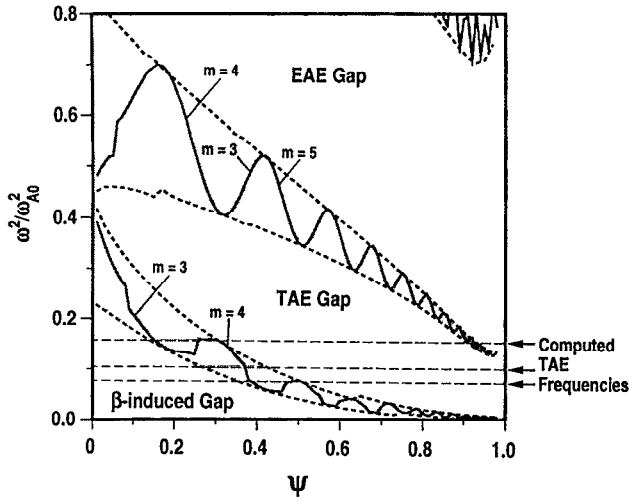

FIG. 3. Computed Alfvén spectrum for discharge 71524 at 1875 msec.

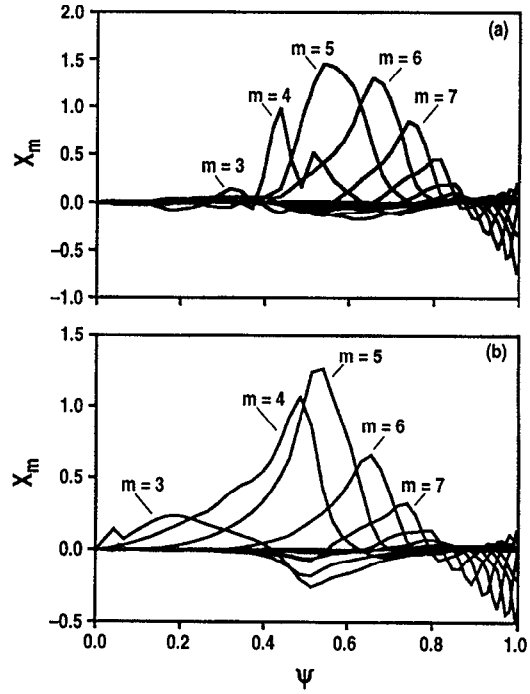

FIG. 4. Poloidal Fourier analysis of computed TAE modes near the observed mode frequencies: (a) $\omega^2=0.076$ and (b) $\omega^2=0.105$, for discharge 71524 at 1875 msec.

accurate reconstructions of the discharge equilibria. These are obtained from the EFITD code[24] which uses external poloidal flux loop and magnetic field probe measurements, internal pressure profile measurements, and multichannel motional Stark effect (MSE) measurements of the internal field line pitch. Also, the location of $q=1$ surfaces, inferred from soft x-ray (SXR) emission profiles, are used to further constrain the fit. The beam pressure profile is obtained from a classical slowing down calculation with the magnitude adjusted to take into account the measured beam loss due to TAE activity. The measured density profile is used both in the pressure profile reconstruction and in the kinetic energy normalization for both the stability codes CONT and GATO. Also, the DIII-D wall, with an ideal resistive vacuum between the plasma boundary and wall, is used as the boundary condition in the GATO stability calculations. The wall is assumed to be ideally conducting.

The spectrum for the 0.8 T discharge (71524), as predicted by the CONT code, is shown in Fig. 3. Here, the solid lines are the loci of the Alfvén resonances for $n=3$; at a given position, there is a singular shear Alfvén mode with the corresponding frequency. The angular frequency ω is normalized to a poloidal Alfvén frequency $\omega_A=(B_0^2/\mu_0 R_0^2\rho_0)^{1/2}/q_0$ where B_0, ρ_0, and q_0 are, respectively, the vacuum magnetic field, the mass density, and the safety factor at the magnetic axis R_0. The dotted lines in Fig. 3 represent the envelopes of the gaps for all n as described in Ref. 17. Acoustic resonances are also present but are not shown.

The GATO code was used to search for $n=3$ TAE modes over the range $0.06\lesssim\omega^2\lesssim 0.18$ which covers most of the TAE gap. Amongst the Alfvén and acoustic modes, three bunches of TAE-like modes were found. The lowest frequency group actually consists of two closely spaced TAE mode frequencies at $\omega^2=0.076$ and 0.081, both of which comprise essentially $m\geqslant 5,6$ TAE modes. The second group of TAE modes, lying near $\omega^2\sim 0.1$, corresponds to the $m=4,5$ TAE mode of the large aspect ratio circular cross-section theories, but with considerable coupling to higher poloidal harmonics. A third group was located at $\omega^2\simeq 0.17$ and corresponds to the $m=3,4$ TAE mode but, again, there is significant coupling to higher harmonics. In this case, however, the frequency intersects the continua near the edge; the lower TAE-like modes, in contrast, cut the continuum only at a smaller minor radius.

The computed TAE mode frequencies for this discharge are shown in comparison to the experimentally measured values in Fig. 2. The two experimental values can clearly be identified with the two lower calculated points. The highest calculated TAE frequency is apparently not observed; this mode is expected to be more strongly damped than the others since it is coupled to the continuum in the high shear region where continuum damping is most effective.

The Fourier-analyzed mode structures for two computed modes close to the observed frequencies are shown in Fig. 4. Here, $X\equiv\xi\cdot\nabla\Psi/|\nabla\Psi|$ and the Fourier analysis is with respect to the PEST poloidal coordinate.[25] The resonances where the TAE mode frequencies cut through the Alfvén continuum in Fig. 3 are typically exhibited in the eigenmode structures as sharp changes in the derivative of the perpendicular component X, reflecting the logarithmic discontinuity.[26] The toroidal coupling of poloidal harmonics outside the resonance ($m\gtrsim 5$), which is characteristic of TAE modes, is clearly seen in both examples.

The lower frequency TAE mode shown in Fig. 4(a) consists of a series of coupled harmonic peaks ranging from $m=5$ to $m\simeq 13$ at the edge. These are coupled inside to the $m=4$ resonant shear Alfvén peak. The higher frequency TAE mode shown in Fig. 4(b), on the other hand,

has a dominant $m=4,5$ TAE-like peak but still with significant coupling to $m \geqslant 5$ nonresonant Fourier harmonics outside, corresponding to the $(m,m+1) \geqslant (5,6)$ local gaps in Fig. 3. The $m=4$ harmonic in this case is sharply peaked as a result of coupling to a nearby acoustic $m=2$ resonance which is not shown in Fig. 3. The $m=4$ peak, however, is not singular.

Calculations were also done for discharge 71515, though in this case the search was made only over the range $0.095 < \omega^2 < 0.15$. Two TAE frequencies were found in these calculations, at $\omega^2 = 0.101$ and 0.133, and these are also shown in Fig. 2. The computed mode structures for that discharge can be seen in Ref. 27. Again, the higher frequency mode, which also corresponds predominantly to the $m=3,4$ TAE mode, clearly cuts the edge continuum and does not appear to correspond to any observed mode. Further experimental confirmation of the importance of continuum damping and the role of shear is given in the following subsection.

B. Damping and thresholds

Considerable theoretical work has gone into the development of alternative damping mechanisms for TAE modes which might account for the original discrepancy with the observed thresholds.[3,4] The approach taken here is to compare the observed thresholds in DIII-D with predictions from the recent published theories. It must be cautioned, however, that all the currently available theories make assumptions—low β, large aspect ratio, circular cross section, and isotropic fast ions in particular—that are rather gross approximations for the DIII-D discharges considered here. The theories are applied in each case by evaluating the one-dimensional expressions for the growth or damping rate, locally across the cross section, using the experimentally determined profiles. The quantitative values should, therefore, not be taken too seriously; the aim is to obtain a qualitative indication of the important physical damping mechanisms and their trends.

In addition to the electron Landau damping and inverse fast-ion Landau drive used in the original estimates,[2] contributions from ion Landau damping have also been shown to be important.[12] Also, a correction factor of $(1+k_\theta \rho_f)^{-1}$, where k_θ is the poloidal wave number and ρ_f is the fast ion gyroradius, has been included in the estimates of the fast-ion driving rate to account for the finite fast-ion Larmor radius. Although recent numerical calculations[28] for the high m limit have shown a rather more complicated dependence on various parameters, the simple, local correction factor used here is adequate for our purposes and is consistent with our basic aim.

Continuum damping occurs when the TAE (or other global mode) frequency intersects with one or more of the shear Alfvén continua; this can occur when the gap structure is sheared as, for example, in Fig. 3. Although more elaborate numerical calculations are again possible,[19,20] the continuum damping rates are estimated from the high m analytic theory described by Rosenbluth *et al.* in Ref. 13. Finally, Mett and Mahajan[15] have shown that the inclusion of finite Larmor radius and a correct treatment of the parallel electric field and electron dynamics, which are essential for the description of the kinetic Alfvén wave (KAW), also lead to important modifications of the TAE. Specifically, the TAE and nearby KAWs can couple and the KAW part can propagate energy away, resulting in enhanced "radiative damping" of the wave.

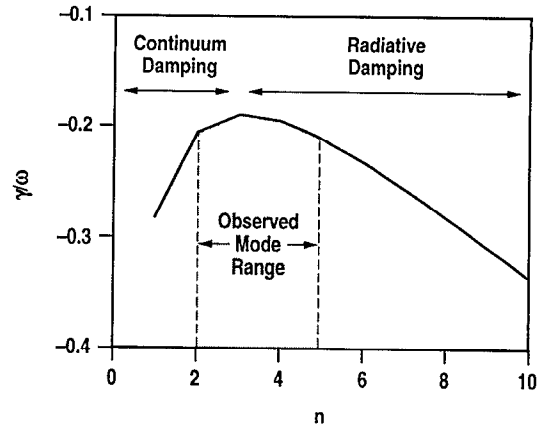

FIG. 5. Computed growth rate for discharge 71524 at 1875 msec as a function of toroidal mode number n.

The predicted and observed thresholds are now qualitatively in agreement, both in gross magnitude and trends.[16] Figure 5 shows the computed total growth rate, including fast-ion drive, for the TAE modes in discharge 71524 at 1875 msec, evaluated at the $q=1.5$ surface, as a function of toroidal mode number n. There is little change in the results if the rates are evaluated anywhere between $q=1$ and 2. This is a case where the TAE modes were marginally destabilized and the computed damping rates exceed the drive by roughly a factor 2, which should be considered good agreement given the gross assumptions made in the theory. The range $2 \leqslant n \leqslant 5$ is also the most unstable, in good agreement with the experimentally observed range of unstable modes.

Further analysis reveals that the radiative damping found in Ref. 15 is the dominant mechanism except for the lowest mode numbers $n \lesssim 3$. In fact, this is the only mechanism considered that is capable of providing a cutoff at high n. For the lowest mode numbers, continuum damping dominates and is probably responsible for the fact that the $n=1$ TAE mode is not usually seen in DIII-D.

Magnetic shear is expected to have a stabilizing effect on TAE modes. The respective theories predict that the continuum damping rate[13] $\gamma_{CD} \propto n^{-3/2} f(S)$ where $f(S)$ is a strong positive function of the shear S, whereas the radiative damping[15] rate $\gamma_{RD} \propto n^{+2/3} S^{2/3}$. (Here, $m \simeq nq$ is assumed.) This suggests that increasing shear ought to preferentially stabilize the low n TAE modes where γ_{CD}, which has a strong shear dependence, is dominant. This is directly confirmed[16] by negative current ramp experiments in which the shear was transiently increased (corresponding to high internal inductance l_i) but slowly relaxed back over a few hundred msec. The results are shown in Fig. 6 for two l_i values, just after the current ramp ($l_i=1.3$) and about 300 msec later ($l_i=1.1$). Once the shear relaxed, the

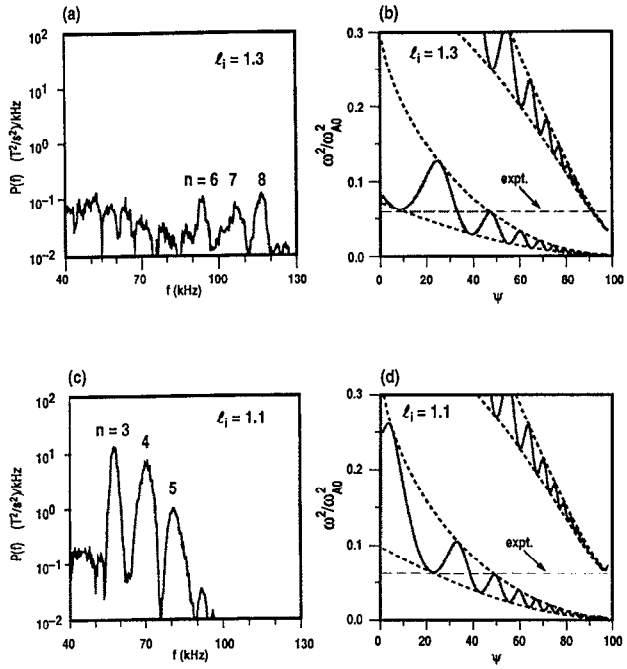

FIG. 6. Measured power spectra (dB_θ/dt) and computed continuum Alfvén spectra for current-ramp experiments: (a) power spectrum and (b) Alfvén spectrum for $l_i=1.3$; (c) power spectrum and (d) Alfvén spectrum for $l_i=1.1$.

TAE amplitude not only increased by an order of magnitude, but the lower n modes became dominant.

The high shear following the negative current ramp has suppressed the low n TAE modes through enhanced continuum damping. This is verified in more detail by analysis of the shear Alfvén spectra in the two cases. Figures 6(b) and 6(d) show the corresponding CONT spectra from an experiment with identical parameters. In the high shear case, the observed mode frequencies cut through the continua near the edge where the shear is large so the low n modes are expected to be strongly damped.[13,16] Although the observed mode frequencies intersect the continuum in the interior, the shear is low in that region and the continuum damping contribution is relatively weak. Later when the edge shear is reduced, the observed mode frequencies no longer intersect the edge continuum so the damping is greatly reduced.

III. BETA-INDUCED ALFVÉN EIGENMODES

At finite β, coupling between compressible acoustic waves and the shear Alfvén modes introduces important modifications to the Alfvén continuum, opening a new β-induced gap at low frequencies.[17] It is found that a new discrete Alfvén-type global mode exists in this gap below the Alfvén continua. This new mode is analogous to the so-called GAE modes[9,10] which appear in cylindrical models at frequencies below the respective continuum branches.

The main effect of including acoustic coupling on the shear Alfvén spectrum, besides the creation of the β-induced gap, is the strong mixing of the acoustic and Alfvén branches in the lower Alfvén continuum. The true eigenmodes of the system in this frequency range are neither pure Alfvén nor pure acoustic and the division between them is somewhat artificial. For our purposes the spectral branches and eigenmodes are divided into "acoustic" and "Alfvén" modes according to the dominant polarization: $|\xi_\parallel| > |\xi_\perp|$ for "acoustic" modes and $|\xi_\perp| > |\xi_\parallel|$ for "Alfvén" modes. Acoustic coupling can be eliminated in both the CONT and GATO codes by imposing $\nabla\cdot\boldsymbol{\xi}=0$ and ignoring the parallel displacement $\xi_\parallel$. With this "incompressible" option, the shear Alfvén spectrum is lowered and the β-induced gap is eliminated. Inclusion of compressibility is therefore crucial, not only to obtaining good agreement with observed frequencies for TAE modes, but also to recovering the new global mode in the β-induced gap.

There is, however, a conceptual difficulty here that needs to be addressed. It is well known that acoustic modes are strongly damped and their propagation is not well described by the MHD model. One might therefore question whether the β-induced gap is an artifact of the full MHD model which does not survive a correct treatment. A distinction needs to be made, however, between the *propagation* of compressional acoustic waves, which are inadequately treated, and the compressional response of the fluid to a propagating *Alfvén* wave, which enters through the geodesic curvature κ_s and finite-β effects.[17] The incompressible option eliminates *all* compressional effects. On the other hand, the so-called slow-sound approximation (SSA),[17] in which $\omega^2 \gg \mu_0\gamma p/\rho_0 R_0^2$, eliminates acoustic wave propagation but retains the compressional response of the fluid to the transverse Alfvén wave; this response is given by[17] $\nabla\cdot\boldsymbol{\xi} = -B^2/(\mu_0\gamma p + B^2)\kappa_s\xi_s$, where $\xi_s = \boldsymbol{\xi}\cdot(\mathbf{B}\times\nabla\Psi)R/|\nabla\Psi|^2$. The associated compressional energy of the Alfvén waves corresponds to an upward shift in frequency from the incompressible model of order β and the β-induced gap is recovered.[17]

In the spirit of the ideal MHD description, the coupling of the compressional fluid response to the Alfvén waves can be retained by either resorting to the SSA, or by using the full MHD model and simply ignoring the acoustic waves, as done here. Both approaches reproduce essentially the same shear Alfvén spectrum and are in agreement with the observed TAE mode spectrum in DIII-D. The incompressible model, on the other hand, does not agree with the observations.

The DIII-D discharges discussed in the previous section all have finite β; 71524, for example, has a normalized β of $\beta_N = \beta/(\mu_0 I/aB) = 3(\beta = 3.7\%)$. Compressibility and acoustic coupling are therefore expected to modify the spectrum for normalized frequencies $\omega^2 \lesssim \beta \sim 0.04$ and it is found that the effect is important in practice for $\omega^2 \lesssim 0.15$ (higher poloidal harmonics of the acoustic spectrum can couple to lower harmonics of the Alfvén spectrum). The crucial point is that compressibility strongly affects the TAE gap but has little effect on the higher gaps. Near the computed TAE frequencies, the nearby acoustic continuum modes generally have some fraction of TAE-like

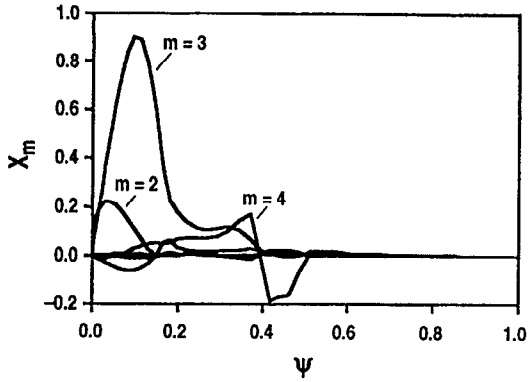

FIG. 7. Poloidal Fourier analysis of the computed BAE mode with $\omega^2=0.072$ for discharge 71524 at 1875 msec.

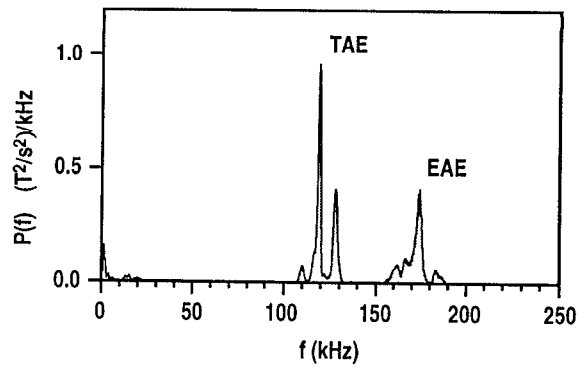

FIG. 8. Power spectrum for discharge 75346 showing TAE and EAE spectra.

Alfvén structure; it is in this sense that the TAE modes occur in bunches. All of the quoted TAE modes, however, have $|\xi_\perp|/|\xi| \gtrsim 0.5$, typically in the same range as that for unstable kink modes.

The presence of the β-induced gap for discharge 71524 at 1875 msec is clearly seen in Fig. 3. Both the calculated and observed TAE mode frequencies cut through this gap in the core. In Fig. 4(b) for the TAE mode at $\omega^2=0.105$, there is also a small but global $m=3$ harmonic inside $\psi=0.4$, which is not expected to be present since this TAE mode lies *below* the $m=3$ continuum branch. A more detailed look at the computed Alfvén eigenmodes reveals several more global modes throughout the observed frequency range, some consisting of an almost pure, global $m=3$ peak extending to varying degrees through the core. An example is shown in Fig. 7 corresponding to $\omega^2=0.0721$. In some cases, this global $m=3$ mode is coupled to a TAE-like component through the resonance.

The eigenmode exhibited in Fig. 7 is best interpreted as a new form of GAE mode since it lies directly under the minimum in the $m=3$ continuum branch. However, it is created only as a result of the finite-β compressional response of the shear Alfvén modes since otherwise the corresponding gap would not exist. For this reason, the new modes are referred to as β-induced Alfvén eigenmodes or BAE's. The polarization of the BAE modes $|\xi_\perp|/|\xi|$ is typically comparable to that of TAE modes in the same frequency range. The BAE modes are therefore Alfvén modes in exactly the same sense as the TAE modes.

The BAE modes are important for the interpretation of the experimental observations discussed in the previous section since they lie in or below the same frequency range as the calculated TAE modes. They may be even more important at higher β. Near the nominal β limit of $\beta_N \sim 3.5$, following an increase in the neutral beam power, the experimentally observed mode frequencies decrease to about one-third of the original frequency. One candidate is the BAE mode; preliminary GATO calculations have shown the existence of BAE modes in the observed lower frequency range. Work on a definitive identification is still underway and will be reported in a future publication.

These new modes could be as important as TAE modes for fast ion loss; coupled BAE and TAE modes could be particularly efficient at expelling the fast particles all the way from the core to the plasma edge. Note that the reason the arguments for the GAE being more strongly damped[2] than the TAE do not apply to the BAE modes is that both the TAE and BAE interact with the same continua. Accurate and comprehensive damping calculations in full noncircular, finite aspect ratio, and finite-β geometry need to be done for both to determine which modes are the more unstable. Ion Landau damping particularly needs to be included since this is likely to be the dominant mechanism for the BAE modes.

IV. THE EAE MODE IN DIII-D

High-frequency fluctuations which cannot be identified with TAE modes or their higher harmonics have been observed in DIII-D discharges. These are believed to be EAE modes. The EAE mode[8] is an isolated global mode, created within an elongation-induced gap from coupling of poloidal harmonics m with $m+2$, at a frequency typically of the order of two to three times the TAE frequency. The magnetic detectors in DIII-D, until recently, were restricted to frequencies below 250 kHz. With the additional Doppler shift from the plasma rotation, this generally puts the expected EAE frequencies outside the detector range. Nevertheless, in a few atypical discharges, high-frequency fluctuations were seen below the 250 kHz cutoff. Figure 8 shows the frequency spectrum for the clearest example (discharge 75346), in which a locked, $n=1$ mode was present which slowed the plasma rotation and reduced the Doppler shift enough so that the higher frequency peaks remained below 200 kHz. The frequencies near 120 kHz are consistent with TAE modes. The peaks near 175 kHz, however, are at too high a frequency to be TAE modes but are in the frequency range expected for EAE modes.

The reconstructed equilibrium profiles are shown superimposed on the Alfvén spectrum in Fig. 9. Although no pressure profile data were available in this or any similar discharges, this was compensated by the availability of a full set of multichannel MSE data. Density profile data were also limited but were sufficient to reconstruct a rea-

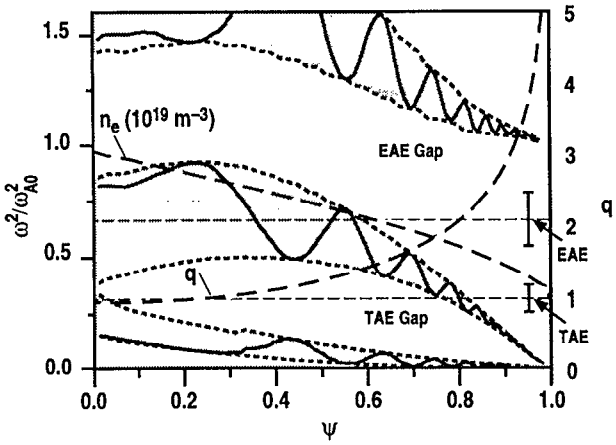

FIG. 9. Reconstructed q and density profiles (long dashes) and Alfvén spectrum showing frequencies of observed TAE and EAE modes for discharge 75346. The $n=3$ Alfvén continuum spectrum is also shown (solid curves) for reference. For this discharge, $B_T=0.8$ T, $I_p=0.5$ MA, $n_e=3\times10^{13}$ cm^{-3}, and $\beta=2\%$. The elongation at the separatrix was $\kappa=1.7$.

sonable equilibrium. The shear Alfvén branches are not shown since the mode number of the largest of the higher frequency peaks is $n=9$ and good numerical resolution of such high mode numbers is difficult to obtain. However, the envelopes of the gaps for all n can be accurately calculated,[17] and these identify the respective gaps adequately. The experimentally observed TAE and EAE frequencies are shown, assuming no Doppler correction. The toroidal mode numbers for the three separate lower frequency TAE peaks were indeterminate, consistent with each peak being a superposition of several toroidal mode numbers in the absence of a Doppler shift. These TAE modes all fall in the TAE gap as expected.

The candidate EAE mode at a normalized frequency given by $\omega^2=0.65$ clearly falls within the expected EAE gap. The error bars shown on the mode frequencies in Fig. 9 are estimated from the error in the density profile reconstruction. Similar errors are also present in the gap envelopes, however, with the largest uncertainty nearest the edge. Even at the extreme of the error bars, the higher frequency modes cannot be made to lie within the TAE gap. Current computer limitations have so far prevented resolution of high mode numbers in the GATO code; hence no GATO calculations have yet been attempted to verify the existence of the EAE mode in this discharge. Nevertheless, GATO calculations at low n for several other discharges, 71524, for example, routinely find several EAE modes lying within the EAE gaps.

V. SUMMARY AND CONCLUSIONS

The results reported in this paper demonstrate a clear convergence between the theory of TAE modes and observations in DIII-D. This is especially true of the real frequency, where the theory predicts, and the observations confirm the presence of multiple modes in the TAE gap, with good quantitative agreement in the individual frequencies. For the damping and thresholds, the agreement is less detailed but the theory and observations are now within a factor of 2 and the ranges of most unstable mode numbers are in good agreement. Moreover, the qualitative trends predicted by the theory are convincingly borne out in current-ramp experiments on DIII-D.

At finite β with compressibility, a new Alfvén mode, the BAE, appears in the lower frequency, β-induced gap. At high β, the experiment indicates a decreasing *observed* frequency with β_N. Note that the reduction in TAE frequency with increasing β predicted from earlier incompressible calculations[29] is too small to account for the observed decrease. The BAE mode, on the other hand, may well explain the observed low-frequency modes. The first definitive observations of the predicted EAE modes were also reported here. This mode was detected by external probes at higher frequency than the TAE mode and the equilibrium reconstruction confirmed that the mode frequency lies in the EAE gap. In more typical DIII-D discharges, the EAE mode may be present but with a mode frequency lying outside the previous detector range.

There are clearly several global Alfvén modes that can be destabilized in high β, shaped discharges. A complete theoretical description of the observed neutral-beam-driven instabilities will require more refined theories of the damping rate that are sensitive to the details of the equilibrium geometry and corresponding gap structure, and to the structure of the eigenmodes. This is clearly important at finite β where the presence of the TAE is complicated by the simultaneous presence of the BAE in the same frequency range. It is even more important at high β_N, where it appears that the TAE modes are stabilized but that unstable modes still persist at lower frequencies. More generally, accurate damping calculations are needed to determine the importance in future devices of TAE, BAE, and EAE modes in all frequency ranges.

ACKNOWLEDGMENTS

The authors wish to acknowledge the many contributions made to this work by the DIII-D Experimental Team. We also wish to acknowledge assistance with the figures from General Atomics' Fusion Publications and Computer Divisions.

This is a report of work sponsored by the U.S. Department of Energy under Contract No. DE-AC03-89ER51114 and Grant No. DE-FG03-92ER54150.

[1] C. Z. Cheng, L. Chen, and M. S. Chance, Ann. Phys. (NY) **161**, 21 (1985); C. Z. Cheng and M. S. Chance, Phys. Fluids **29**, 3695 (1986).
[2] G. Y. Fu and J. W. Van Dam, Phys. Fluids B **1**, 1949, 2404 (1989); L. Chen, in *Theory of Fusion Plasmas*, Proceedings of the 1988 International Workshop, Varenna–Lausanne, 1987, edited by J. Vaclavik, F. Troyon, and E. Sindoni (Editrice Compositori, Bologna, 1988), p. 327; L. Chen, R. B. White, G. Rewoldt, P. L. Colestock, P. H. Rutherford, M. N. Bussac, Y. P. Chen, F. J. Ke, and S. T. Tsai, in *Proceedings of the 12th International Conference on Plasma Physics and Controlled Nuclear Fusion Research, 1988*, Nice (International Atomic Energy Agency, Vienna, 1989), Vol. II, p. 77.
[3] W. W. Heidbrink, E. J. Strait, E. Doyle, G. Sager, and R. Snider, Nucl. Fusion **31**, 1635 (1991).
[4] K. L. Wong, R. J. Fonck, S. F. Paul, D. R. Roberts, E. D. Fredrickson,

R. Nazikian, H. K. Park, M. Bell, N. L. Bretz, R. Budny, S. Cohen, G. W. Hammett, F. C. Jobes, L. Johnson, D. M. Meade, S. S. Medley, D. Muller, Y. Nagayama, D. K. Owens, and E. J. Synakowski, Phys. Rev. Lett. **66**, 1874 (1991).
[5]H. H. Duong, W. W. Heidbrink, E. J. Strait, C. T. Hsu, R. Lee, T. W. Petrie, A. D. Turnbull, R. Moyer, and J. Watkins, "Loss of beam ions during TAE instabilities," to appear in Nucl. Fusion; H. H. Duong and W. W. Heidbrink, "Confinement of fusion-produced MeV ions in the DIII-D tokamak," Nucl. Fusion **33**, 211 (1993).
[6]J. P. Goedbloed, Phys. Fluids **18**, 1258 (1975); O. P. Pogutse and E. I. Yurchenko, Nucl. Fusion **18**, 1629 (1978).
[7]R. L. Dewar, R. C. Grimm, J. L. Johnson, E. A. Frieman, J. M. Greene, and P. H. Rutherford, Phys. Fluids **17**, 930 (1974).
[8]R. Betti and J. P. Friedberg, Phys. Fluids B **3**, 1865 (1991).
[9]A. Pochelon, R. Keller, F. Troyon, and R. Gruber, in *Proceedings of the 7th European Conference on Controlled Fusion and Plasma Physics*, Lausanne (European Physical Society, Petit-Lancy, Switzerland, 1975), Vol. 1, p. 157; D. W. Ross, G. L. Chen, and S. M. Mahajan, Phys. Fluids **25**, 652 (1982); A. de Chambrier, A. D. Cheetham, A. Heym, F. Hofmann, B. Joye, R. Keller, A. Lietti, J. B. Lister, and A. Pochelon, Plasma Phys. **24**, 893 (1982).
[10]K. Appert, R. Gruber, F. Troyon, and J. Vaclavik, Plasma Phys. **24**, 1147 (1982); S. M. Mahajan, D. W. Ross, and G. L. Chen, Phys. Fluids **27**, 2238 (1984).
[11]Y. M. Li, S. M. Mahajan, and D. W. Ross, Phys. Fluids **30**, 1466 (1987).
[12]R. Betti and J. P. Friedberg, Phys. Fluids B **4**, 1465 (1992); H. Biglari, F. Zonca, and L. Chen, *ibid.* **4**, 2388 (1992).
[13]M. N. Rosenbluth, H. L. Berk, J. W. Van Dam, and D. M. Lindberg, Phys. Rev. Lett. **68**, 596 (1992); M. N. Rosenbluth, H. L. Berk, J. W. Van Dam, and D. M. Lindberg, Phys. Fluids B **4**, 2189 (1992); H. L. Berk, J. W. Van Dam, Z. Guo, and D. M. Lindberg, *ibid.* **4**, 1806 (1992).
[14]F. Zonca and L. Chen, Phys. Rev. Lett. **68**, 592 (1992).
[15]R. R. Mett and S. M. Mahajan, Phys. Fluids B **4**, 2885 (1992).
[16]E. J. Strait, W. W. Heidbrink, M. S. Chu, H. H. Duong, L. L. Lao, A. D. Turnbull, and the DIII-D Team, "Stability of TAE modes in DIII-D," to appear in *Proceedings of the 14th International Conference on Plasma Physics and Controlled Nuclear Fusion Research, 1992*, Würzburg (International Atomic Energy Agency, Vienna, in press); E. J. Strait, W. W. Heidbrink, A. D. Turnbull, M. S. Chu, and H. H. Duong, "Stability of neutral beam-driven TAE modes in DIII-D," submitted to Nucl. Fusion.
[17]M. S. Chu, J. M. Greene, L. L. Lao, A. D. Turnbull, and M. S. Chance, Phys. Fluids B **4**, 3713 (1992).
[18]C. Z. Cheng, Phys. Fluids B **3**, 2463 (1991).
[19]L. Villard and G. Y. Fu, Nucl. Fusion **32**, 1695 (1992).
[20]S. Poedts, W. Kerner, J. P. Goedbloed, B. Keegan, G. T. A. Huysmans, and E. Schwarz, Plasma Phys. Controlled Fusion **34**, 1397 (1991); D. A. Spong, B. A. Carreras, and C. L. Hedrick, Phys. Fluids B **4**, 3316 (1992).
[21]J. L. Luxon and L. G. Davis, Fusion Technol. **8**, 441 (1985).
[22]H. Biglari and L. Chen, Phys. Rev. Lett. **67**, 3681 (1991).
[23]L. C. Bernard, F. J. Helton, and R. W. Moore, Comput. Phys. Commun. **24**, 377 (1981).
[24]L. L. Lao, J. R. Ferron, R. J. Groebner, W. Howl, H. St. John, E. J. Strait, and T. S. Taylor, Nucl. Fusion **30**, 1035 (1990); D. Wroblewski and L. L. Lao, Phys. Fluids B **3**, 2877 (1991).
[25]R. C. Grimm, J. M. Greene, and J. L. Johnson, in *Methods in Computational Physics*, edited by J. Killeen (Academic, New York, 1976), Vol. 16, p. 253.
[26]A. D. Turnbull, M. S. Chu, M. S. Chance, J. M. Greene, L. L. Lao, and E. J. Strait, Phys. Fluids B **4**, 3451 (1992).
[27]A. D. Turnbull, M. S. Chu, E. J. Strait, W. W. Heidbrink, H. Duong, L. L. Lao, J. M. Greene, M. S. Chance, and T. S. Taylor, in *Proceedings of the 13th European Conference on Controlled Fusion and Plasma Physics*, Innsbruck (European Physical Society, Petit-Lancy, Switzerland, 1992) Vol. 16C, Part 1, p. 435.
[28]G. Y. Fu and C. Z. Cheng, Phys. Fluids B **4**, 3722 (1992).
[29]G. Y. Fu and C. Z. Cheng, Phys. Fluids B **2**, 985 (1990).